Arab J Sci Eng (2016) 41:2611–2621
DOI 10.1007/s13369-016-2109-3

RESEARCH ARTICLE - CHEMICAL ENGINEERING

Comparative Study Between Response Surface Methodology and Artificial Neural Network for Adsorption of Crystal Violet on Magnetic Activated Carbon

Iman Salehi[1] · Mahboube Shirani[1] · Abolfazl Semnani[1] · Mohsen Hassani[2] · Saeed Habibollahi[3]

Received: 1 December 2015 / Accepted: 15 March 2016 / Published online: 28 March 2016

Abstract The easily separable and regenerable magnetic activated carbon was synthesized for adsorption of toxic cationic dye, crystal violet, from aqueous solution. The synthesized magnetic activated carbon was characterized by SEM–EDX. The magnetic property of sorbent was evaluated by VSM method. The obtained saturation magnetization of 41.56 emu g^{-1} showed facile separation of sorbent after adsorption process. The effect of five parameters of pH, temperature, time, initial dye concentration and sorbent amount on adsorption (%) were investigated. The percentage of adsorption was mathematically described as a function of experimental parameters and was estimated by central composite design (CCD). The maximum adsorption percent of 99.5 ± 0.2 was obtained experimentally which was close to the percent of CCD prediction of 99.90 %. The same design was used for a three-layer artificial neural network model (ANN). The predicted data of CCD versus ANN showed the linear agreement with regression value (R^2) of 0.9994 which confirmed the ideality of CCD and ANN. The results of two models were compared in terms of coefficient of determination (R^2) and mean absolute percentage error (MAPE) to indicate the prediction potential of CCD and ANN. The MAPE (%) of 0.59 and 0.38 was found for CCD and ANN respectively. The obtained results indicated higher capability and accuracy of ANN in prediction. The experimental data were found to be properly fitted to the Langmuir and Freundlich models which indicates that the sorption takes place on a heterogeneous material and the sorption capacity of 12.59 mg g^{-1} was achieved.

Keywords Adsorption · Crystal violet · Magnetic activated carbon · Central composite design · Artificial neural network

1 Introduction

In recent years releasing toxic dyes by different industries (textile, printing, cosmetic, food, and etc.) into water sources such as rivers, lakes, and seas has been a considerable concern due to water pollution and aquatic living organism death. Water pollution is one of the most threatening factors of human health. Aggregation of dyes in water causes cancer, genetic mutation, digestive disorders, and poisoning. Crystal violet (Scheme 1) is one of the most common cationic dyes which is utilized in all dye industries. Crystal violet is very toxic to aquatic organisms. It is harmful to the embryo and can cause genetic mutation. Accumulation of crystal violet in body can lead to gastrointestinal tract irritation with nausea, vomiting, hypermobility, abdominal pain, and respiratory problems [1,2]. Therefore, due to the dangerous health effect of crystal violet, removal of such toxic dye becomes necessary. Various techniques such as oxidative degradation [3], electrocoagulation [4], coagulation [5], membrane filtration [6] and ozonation [7] have been reported for toxic dyes removal from aqueous solutions. However, adsorption grabs scientists' attention among all removal methods due to the

Electronic supplementary material The online version of this article (doi:10.1007/s13369-016-2109-3) contains supplementary material, which is available to authorized users.

✉ Abolfazl Semnani
a.semnani1341@gmail.com

[1] Department of Chemistry, Faculty of Science, Shahrekord University, P.O. Box 115, Shahrekord, Iran

[2] Department of Mechanical Engineering, Najafabad Branch, Islamic Azad University, Isfahan, Iran

[3] Department of Chemistry, Payame Noor University, P.O.Box 19395-4697, Tehran, Iran

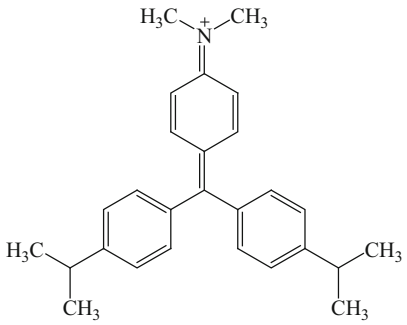

Scheme 1 Chemical structure of crystal violet

advantages of simplicity, low-cost adsorbents, easy industrialization, facile accessibility. Zeolite, active carbon, alumina, are widely used for removal of different dyes. Application of magnetic sorbents has made a revolution in adsorption techniques in recent years due to the advantages of easier and faster separation of sorbent from the sample solution by an external magnet. In this research the toxic cationic dye of crystal violet was adsorbed by magnetic activated carbon.

In order to save time and money, statistical and mathematical models have been used to estimate and simulate the conditions in different processes especially in chemistry. Response surface methodology (RSM) and artificial neural network (ANN) are two powerful models which are widely applied to predict the processes in chemistry. Artificial neural network is a representative of human brain system in which the interconnected neurons and their exchange messages between each other are considered. ANN is successfully applied for both linear and nonlinear systems [8,9]. Among all statistical models, ANN is one of the most prevalent models for nonlinear analysis. Determination of complicated nonlinear relationships between input variables and prediction of output variables can be gained by ANN model. ANN has been reported for adsorption of crystal violet [10]. RSM deals with a group of mathematical and statistical techniques in order to fit predicted model to the experimental data obtained in relation to experimental design and obtain the optimum parameters. RSM is a powerful method for prediction of large number of processes which is applied in two common designs of Box–Behnken design and central composite design [11]. Many studies have been reported in which RSM and ANN both were applied to predict and optimize the process [12–16]. The results in these studies showed higher potential and ability of ANN in prediction and optimization comparing to RSM. For instance, Khayet et al. [17] applied RSM and ANN modeling and optimization of desalination process by reverse osmosis. They showed that RSM was not efficient and useful the proposed method of reverse osmosis over a wide range of salt concentration in feed solution. However, ANN was completely and powerfully successful in modeling and optimization of desalination process by reverse osmosis.

Adsorption of crystal violet was reported by different sorbents using RSM [18,19]. In this study, adsorption of crystal violet by magnetic active carbon from aqueous solutions was investigated. The process was considered applying two potent statistical models of RSM and ANN and the coefficient of determination (R^2) and mean absolute percentage error (MAPE) of RSM and ANN were compared.

2 Experimental

2.1 Regents

All the chemicals [i.e., crystal violet ($C_{25}N_3H_{30}Cl$), hydrochloric acid, sodium hydroxide, deionized water, iron (II) sulfate heptahydrate, and activated carbon] used in this study were analytical grade with the highest purity available and they were purchased from Merck.

2.2 Apparatus

The pH measurements were done with 86502-pH/ORP (AZ Instrument, Taiwan) using a combined glass calomel electrode. Ultrasonic bath (Sonorex digitec, DT255H, Germany) and oven (Universal model UF 55, Germany) both were utilized for magnetic activated carbon preparation. IKA overhead stirrer (model RW 28 Digital Package, Germany) with glass stirrer was applied to stir the magnetic sorbent sample solution during adsorption process. Ultrospec 3100 pro UV-Visible spectrophotometer (Amersham Biosciences, USA) was carried out for data analyzing. A vibration-sample magnetometer (Meghnatis Daghigh Kavir Co.) was used to characterize the magnetic properties of synthesized magnetic activated carbon.

2.3 Preparation of Magnetic Activated Carbon

Magnetic activated carbon was prepared according to the proposed procedure [20]. Briefly, 2.78 g of iron (II) sulfate heptahydrate was dissolved in deionized water. Then 0.5 g of fine activated carbon powder was added to the solution. Ten milliliters solution of NaOH 2.5 mol L^{-1} was added dropwise to the mixture. The mixture was stirred at 100 °C for 1 h. The obtained magnetic sorbent was washed with deionized water for several times. Finally, the obtained magnetic activated carbon was dried at 50 °C in the oven.

2.4 Adsorption Procedure

Ten milliliters of crystal violet solution was adjusted at the proper values of pH, temperature, time, initial dye concen-

tration, and amount of magnetic activated carbon, based on the predicted conditions of CCD experimental design runs. After the certified time, the magnetic activated carbon was separated from the solution by an external magnet, and the upper aqueous phase was determined by UV–visible spectrophotometer.

The uptake of adsorbate can be mathematically figured out by Eq. 1 as follows [21]:

$$Q_i = (C_\mathrm{i} - C_\mathrm{e})\,/S \tag{1}$$

Q_i the adsorbate concentration adsorbed at the equilibrium (mg of adsorbate/g of adsorbent), C_i the initial dye concentration in the solution (mg L^{-1}), C_e equilibrium concentration or final dye concentration (mg L^{-1}), Sdosage concentration which is obtained as following (Eq. 2)

$$S = m/v \tag{2}$$

where m is the adsorbent mass (g) and v is the volume of adsorbate solution (L).

Finally the percentage of adsorption percentage can be stated according to the following equation (Eq. 3):

$$\text{Dye removal percentage}\,(\%) = (C_\mathrm{i} - C_\mathrm{e})\,/C_\mathrm{i} \times 100 \tag{3}$$

2.5 Experimental Design Models

2.5.1 Response Surface Methodology

There are various kinds of statistical methods to analyze chemical processes. Some of these methods are used to predict the conditions in a process. Response surface methodology (RSM) is one of the most common factorial designs used for statistical analysis. RSM is based on the fit of empirical models to the experimental data obtained from experimental design [11,22]. RSM is composed of two designs of two designs of central composite design (CCD) and Box–Behnken design (BBD). Experimental design of central composite design (CCD) as a partial factorial design was applied to predict the present study conditions. MINITAB software version 16.0 was used for the experimental design to optimize the dominant parameters of pH (in the range of 4.5–10.5 with 0.5 intervals), temperature (25–65 °C with ten intervals), time (5–45 min with ten intervals), initial dye concentration (5–45 mg L^{-1} with ten intervals) and the amount of sorbent (15–75 mg with 15 intervals) on dye removal percentage. The coded setting data for parameters were −2, −1, 0, +1, +2. Three replications at the center of the design were applied to determine the precision of the method. A full quadratic equation was used to depict the interaction of the factors in the process as the following (Eq. 4):

$$Y = b_0 + \sum_{i=1}^{k} b_i x_i + \sum_{i=1}^{k} b_{ii} x_i^2 + \sum_{i}^{i<j} \sum_{j} b_{ij} x_i x_j \tag{4}$$

where the Y is the predicted response and b_o, b_i, b_{ii}, and b_{ij} are the regression coefficients for the intercept, linearity, square, and interaction terms, respectively, and x_i and x_j are the coded independent variables.

2.5.2 Artificial Neural Network

Neural Network Toolbox Version 6.0.4 of MATLAB® R2010 was utilized to predict the proposed procedure. A three-layer ANN with tan-sigmoid, and purline function was used for hidden and output layers as transfer functions, respectively. The tan-sigmoid transfer function was exposed as follows [23]:

$$F(x) = 1/(1 + \exp(-x)) \tag{5}$$

In order to minimize the mean-squared error, training network is applied on any ANN modeling. To this aim, feed forward back propagation (FFBP) was used as training algorithm in this study. In this process, the final calculated outputs are compared with the experimentally obtained outputs, and the errors are estimated. These errors are then propagated backwards and used for adjusting the weights of neurons. It should be mentioned that the weights of the trained network are stored, and can be applied later for the outputs prediction of a different set of inputs. Thirty-two experimental data, obtained from CCD, were applied as input data in ANN modeling for five input variables of pH, temperature, time, initial dye concentration and amount of sorbent. Twenty-six and six data points were derived to training and test sets respectively. Data points in ANN were normalized in the range of $[-0.9, 0.9]$ by using tan-sigmoid transfer function as follows:

$$X_\mathrm{norm} = 1.8\,(X - X_\mathrm{min})\,/\,(X_\mathrm{max} - X_\mathrm{min}) - 0.9 \tag{6}$$

where X is variable, X_min, X_max are minimum and maximum values respectively.

3 Results and Discussion

3.1 Characterization of Magnetic Activated Carbon

The SEM image of magnetic activated carbon is shown in Fig. 1, which indicates the nanostructure of the sorbent. The chemical composition of magnetic activated carbon, taken by EDX, is shown in Fig. 2. The vibrating sample magnetometer analysis (VSM) was applied to prove the magnetic properties and the required force to move magnetic activated

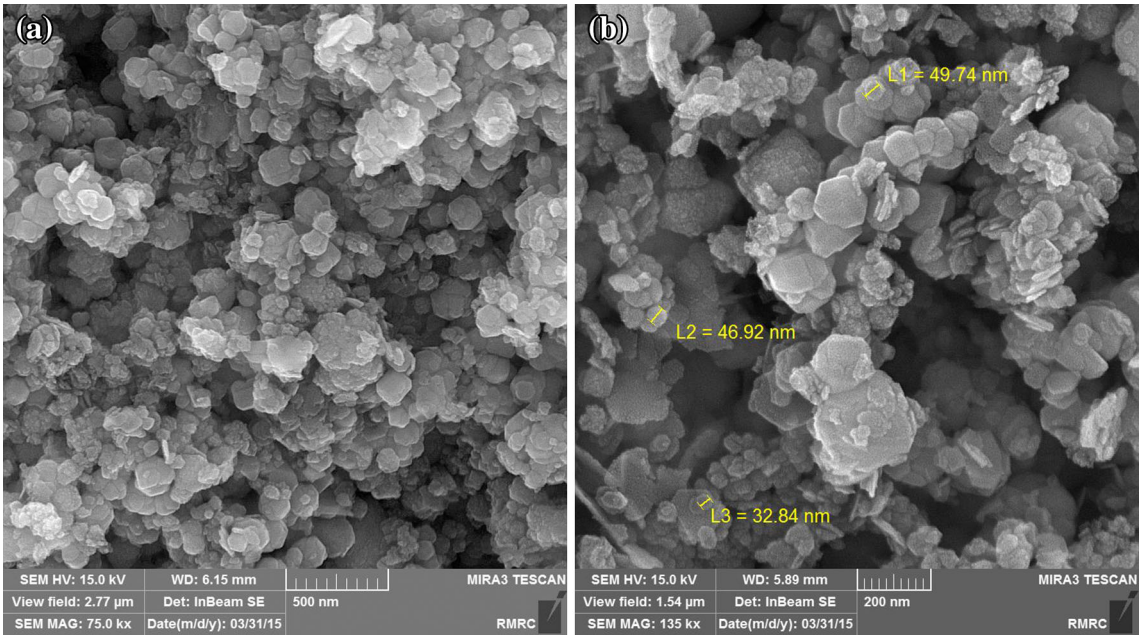

Fig. 1 The SEM image of magnetic activated carbon. **a** 500 nm *scale*, **b** 200 nm

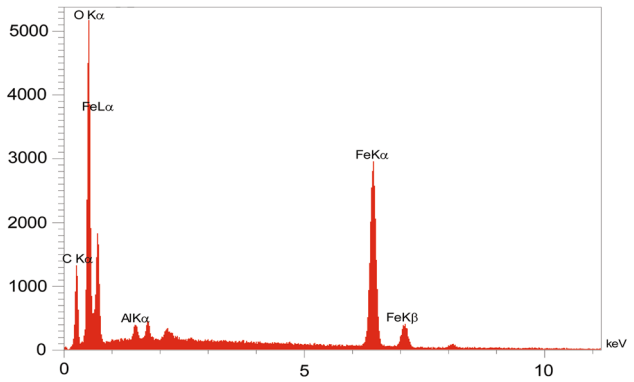

Fig. 2 EDX image of magnetic activated carbon

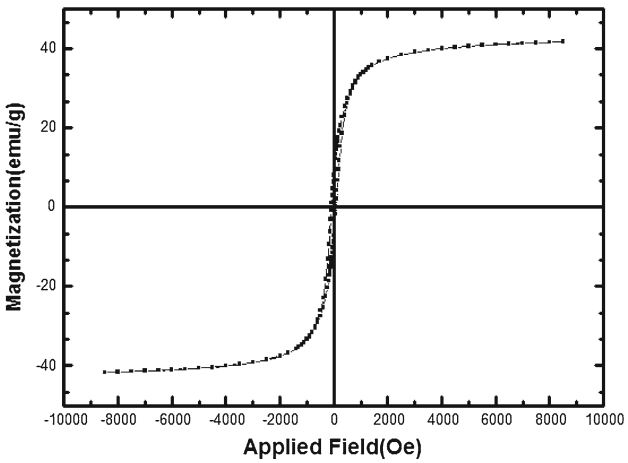

Fig. 3 The hysteresis loops of magnetic activated carbon

carbon from solution. The magnetic curve in Fig. 3 shows appropriate super paramagnetic property of magnetic activated carbon due to no hysteresis loop and no eminence existence. While the magnetic activated carbon was exposed to an external magnetic field reserves no magnetization and redisposed after magnetic field removal. The saturation magnetization of 41.56 emu g^{-1} at 298 K was observed which indicated the attraction of magnetic activated carbon by an external magnet.

3.2 CCD Modeling

The adsorption percent of crystal violet as a function of the independent variables within the region of investigation is stated by Eq. 6:

$$\begin{aligned} Y = {} & -2.0408 + 19.703x_1 + 0.672x_2 + 0.561x_3 \\ & - 2.007x_4 + 1.253x_5 - 1.082x_1^2 - 0.005x_3^2 \\ & - 0.010x_4^2 - 0.016x_5^2 - 0.088x_1x_2 - 0.01x_3x_5 \\ & + 0.009x_3x_4 - 0.037x_4x_5 \end{aligned} \tag{7}$$

The predicted and experimental responses of CCD model for 32 runs are indicated in Table 1. Considering the optimum predicted conditions of pH of 9.5, temperature of 25 °C, time of 36 min, initial dye concentration of 19.8 mg L^{-1}, and magnetic activated carbon amount of 52.8 mg, maximum adsorption percent of 99.90 % was obtained. Analysis of experimental data was carried out by response surface design (RSD) using Minitab software. The *p* values for all

Table 1 Experimental matrix for five-level–five factors CCD for adsorption of crystal violet

Exp. no.	Factors						Adsorption (%)	
	pH	Temperature (°C)	Time (min)	Initial dye con. ($mg\,L^{-1}$)	MAC amount (mg)	Obtained	Predicted	
							CCD	ANN
1	6	55	35	35	30	77.60	78.03	77.88
2	9	55	15	35	30	68.43	68.33	68.36
3	6	35	35	15	30	98.33	97.82	98.00
4	9	35	35	15	60	100.31	99.80	99.98
5	7.5	45	25	25	45	98.72	99.31	99.10
6	7.5	45	25	25	45	99.71	99.31	99.45
7	7.5	65	25	25	45	99.75	99.88	99.83
8	7.5	45	25	45	45	84.60	82.98	83.55
9	6	35	15	15	60	100.29	100.06	100.14
10	9	35	35	35	30	77.65	77.63	77.64
11	6	35	15	35	30	67.72	67.99	67.90
12	7.5	45	25	25	45	99.72	99.31	99.45
13	9	55	35	35	60	95.46	95.90	95.75
14	7.5	45	25	25	45	99.64	99.31	99.43
15	7.5	45	25	5	45	105.80	107.82	107.11
16	6	55	15	15	30	98.16	97.56	97.77
17	9	35	15	35	60	97.50	97.77	97.68
18	7.5	45	5	25	45	94.78	95.23	95.07
19	9	35	15	15	30	95.65	94.60	94.97
20	9	55	35	15	30	96.55	95.66	95.97
21	7.5	45	25	25	45	99.48	99.31	99.37
22	7.5	45	45	25	45	99.69	99.65	99.66
23	6	35	35	35	60	98.76	99.57	99.29
24	7.5	45	25	25	15	69.40	70.43	70.07
25	10.5	45	25	25	45	87.01	88.04	87.68
26	7.5	25	25	25	45	99.37	99.65	99.55
27	9	55	15	15	60	100.33	99.73	99.94
28	4.5	45	25	25	45	91.80	91.18	91.40
29	7.5	45	25	25	45	98.99	99.31	99.20
30	6	55	35	15	60	100.24	100.17	100.20
31	6	55	15	35	60	100.10	100.82	100.57
32	7.5	45	25	25	75	100.09	99.48	99.69

variables in the model are all <0.05, which are indicative explanation for ideal prediction of CCD for the process with a linear relationship between the variables. The p values for all variables in the model which are >0.05, reveal the non-linear relationship between the interest variables and for all p values >0.05, the related variables would be removed from the model equation for the process. In each run, the predicted results were obtained by substituting the coefficients and numerical values of the variables in Eq. 6. The linear regression coefficients (R^2) of 0.9953 for the predicted data versus experimental data proved good agreements between predicted and experimental responses. The adjusted R^2 was 98.74 %, which proved the competence of the developed model to predict the proposed process.

3.3 Effect of Variables on Dye Removal

The effect of five parameters of pH, temperature, time, initial dye concentration, and amount of magnetic activated carbon on dye removal and their interactions were investigated. The obtained results from CCD modeling are shown in Fig. 4.

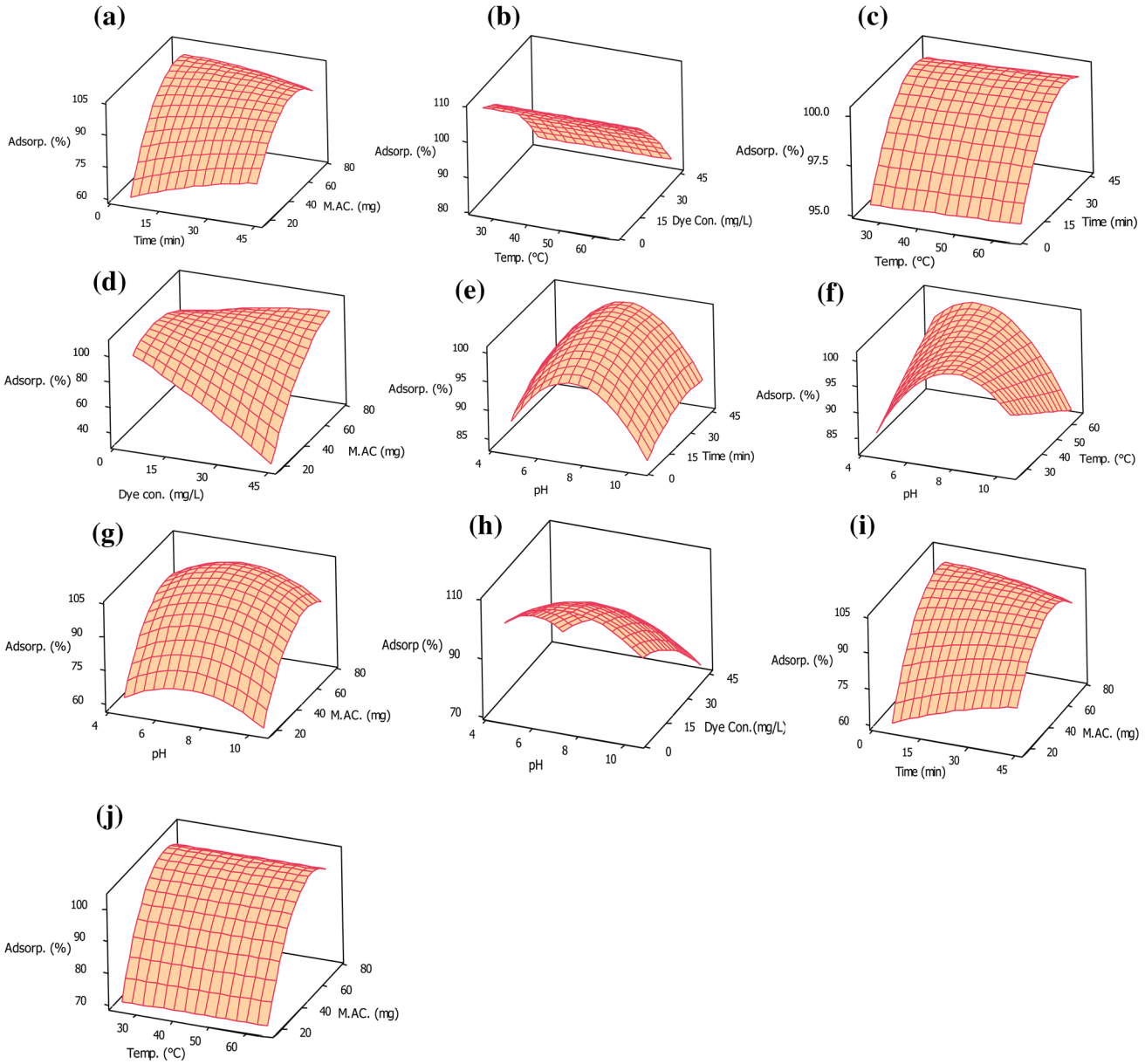

Fig. 4 The surface plots: showing the effect of five interest parameters on the percent of crystal violet adsorption at optimum conditions of 9.5, 25 °C, 36 min, 19.8 mg L^{-1}, and 52.8 mg, for pH, temperature, time, initial dyes concentration, and adsorbent mass

3.3.1 The Effect of pH

pH is a representative of acidity or basicity of the solution and is a significant factor in the dye adsorption process due to the nature of cationic or anionic base of dyes. The effect of pH was studied in the range of 4.5–10.5, using hydrochloride acid and sodium hydroxide. The results in Fig. 4e–h shows that as the pH solution increased to 9.5, the adsorption (%) increased and remained constant up to 9.5. Therefore, the optimum pH of 9.5 was chosen for the process. It seems that at basic conditions (high pH), the surface of adsorbent becomes negatively charged which intensifies the electrostatic interaction and attraction of cationic dye (crystal violet) on the negative surface of the adsorbent. At low pH, there will be a tough competition between proton and the cationic dye for adsorbing on the magnetic activated carbon.

3.3.2 The Effect of Temperature

Temperature is one of the most indicative factors in adsorption. Generally, considering the type of dye (cationic or anionic dyes), adsorption can represent exothermic or endothermic [24]. While the increase in temperature leads to adsorption percent enhancement, the adsorption process is

endothermic. In other word, the adsorption capacity increases as the temperature enhances which indicates the endothermic nature of the adsorption process. The adsorption of cationic dyes is mainly endothermic. Since crystal violet is a cationic dye, this statement came true for it. It seems that by increasing the temperature, the mobility of the dye molecules increase in a parallel manner which results in more adsorption on the surface. The effect of temperature was investigated in the range of 25–65 °C. As shown in Fig. 4b, c, f, j, by increasing the temperature a very slight increase was observed in percent of adsorption which can be neglected. Therefore, for ease of process, the optimum temperature of 25 °C was considered.

3.3.3 The Effect of Time

Achieving to the equilibrium state is a key factor in all chemical processes. The equilibrium between aqueous solution and sorbent can definitely effect the adsorption percent. Therefore, the adsorption time was investigated in the range of 5–45 min. As shown in Fig. 4a, c, e, i, by increasing the contact time, the adsorption (%) increases to 36 min and remains constant in the range of 36–45 min due to the more accomplishment of the adsorption. Hence, the optimum time of 36 min was achieved for further studies.

3.3.4 The Effect of Initial Dye Concentration and Amount of Sorbet

Initial dye concentration is an influential parameter in adsorption process. The effect of initial dye concentration was studied in the range of 10–50 mg L^{-1}. The increase in dye concentration causes active sites saturation on the magnetic activated carbon. According to the surface plots in Fig. 4b, d, e, adsorption percent is nearly constant from 10 to 19.8 mg L^{-1} and up to 19.8 mg L^{-1} a decreasing trend is observed. Therefore, the optimum dye concentration of 10–19.8 mg L^{-1} was considered for the process. Consequently, it can be stated that the more the amount of sorbet is the more the vacant and unoccupied sites are on the adsorbent structure to adsorb the dye molecules and also the more contact surface will be provided. According to the obtained results in Fig. 4a, d, g, i, j, the adsorption percent has an increasing trend to 52.8 and up to it the adsorption percent remains almost constant. Therefore, the optimum sorbent amount of 52.8 mg was selected for the process.

3.4 ANN Modeling

The input variables of trained ANN are pH, temperature (Temp.), time, initial dye concentration (Conc.), and amount of magnetic activated carbon (MAC) and the output is adsorption efficiency of crystal violet. The number of layers, neurons of each layer, and their interconnects are shown in the topology of ANN in Fig. 5. The predicted values by ANN are indicated in Table 2. The regression analysis between experimental data and predicted data by ANN indicated R^2 value of 0.9980 which showed acceptable and reasonable agreements between predicted and experimental responses. The most important purpose of ANN training is to acquire the ideal weights with minimum values of prediction error.

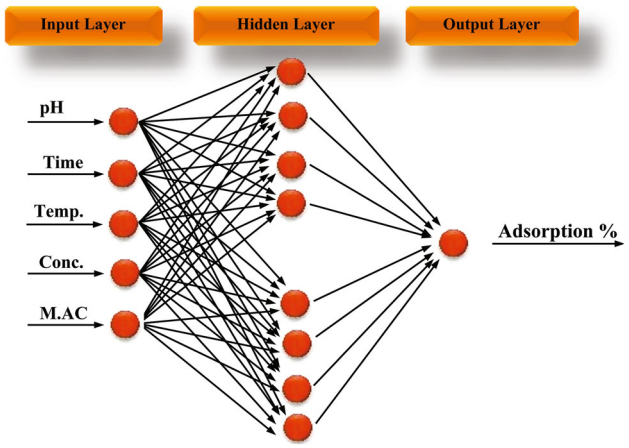

Fig. 5 Optimized topology of artificial neural network

Minimum prediction error was obtained by altering the number of neurons in hidden layer, transfer functions and repetition of training step. In order to find the appropriate number of neurons in hidden layer, various topologies were considered. The applied artificial neural network with eight neurons in hidden layer has the minimum value of mean square error (MSE). The most efficient experimental model provides the minimum MSE. The MSE function equation is as follows:

$$\mathrm{MSE} = \frac{1}{N}\sum_{i=1}^{N}\left(Y_{\mathrm{pre}} - Y_{\mathrm{ex}}\right)^2 \tag{8}$$

where Y_{ex} is the experimental output, Y_{pre} is the network output and N is the number of data points [25]. The accuracy of ANN was investigated by using test data set (Table 2). The values of MAPE were acquired 0.38 % which reveals high accuracy of the ANN model for process.

3.5 Comparison of CCD and ANN Models

CCD and ANN are as two powerful prediction models which widely applied in many chemical processes with linear and nonlinear multivariate regression problems [17]. ANN and CCD were successfully utilized for adsorption of crystal violet by magnetic activated carbon. In order to assess the suitability of ANN and CCD in the proposed process, the MAPE (%) values and the determination coefficients

Table 2 Comparative results of the experiment and predicted values by ANN and CCD for test data set

No.	Factors					Adsorption (%)			APE (%)	
	pH	Time (min)	Temp. (°C)	Initial dye con. (mg L^{-1})	MAC amount (mg)	Exp.	ANN	CCD	ANN	CCD
1	6	35	35	15	30	98.33	98.00	97.82	0.34	0.52
2	9	35	35	35	30	77.65	77.64	77.63	0.02	0.03
3	7.5	5	45	25	45	94.78	95.07	95.23	0.31	0.47
4	10.5	25	45	25	45	87.01	87.68	88.04	0.77	1.18
5	9	15	55	15	60	100.33	99.94	99.73	0.39	0.60
6	6	15	55	35	60	100.10	100.57	100.82	0.47	0.72
MAPE (%)									0.38	0.59

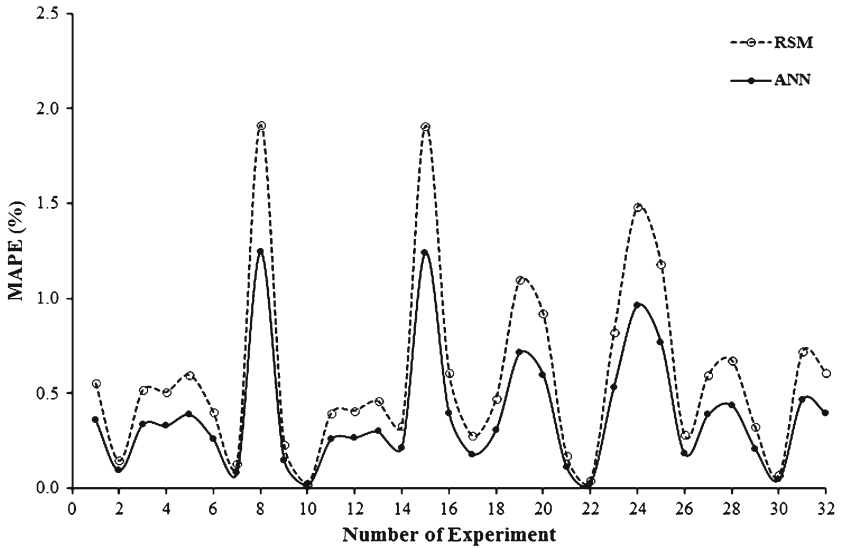

Fig. 6 MAPE (%) of RSM (CCD) and ANN versus number of experiments

(R^2) of two models were compared (calculated according to Eq. 8) [26].

$$R^2 = 1 + \frac{\sum_{i=1}^{n} (y_i - y_{di})^2}{\sum_{i=1}^{n} (y_{di} - y_m)^2} \tag{9}$$

where n is the number of points, y_i is the predicted value, y_{di} is the experimental value, and y_m is the average of the experimental values. The MAPE (%) of 0.59 and 0.38 were found for RSM (CCD) and ANN, respectively. Figure 6 shows the MAPE (%) of RSM (CCD) and ANN versus number of experiments. the MAPE value of RSM model is obviously more than ANN model for each experimental test. Hence, the accuracy of ANN model is higher than RSM model. The coefficients of determination of 0.9953 and 0.9980 were obtained for CCD and ANN model, respectively. R^2 is an indicative to show the prediction potential of the model for the process. Although according to the results, both CCD and ANN could ideally estimate the process, ANN is more dominant and efficient than CCD in prediction. RSM can only model based on the quadratic nonlinear correlation, since ANN can overcome this drawback and consider any form of nonlinearity.

3.6 Regeneration of Adsorbent

The most prominent benefit of the proposed sorbent was its easy separation from the media and reusability. The used sorbent can be regenerated by a suitable solvent. The regeneration of the sorbent was considered by methanol, ethanol, and acetone. The desorption percent of 94.5, 75.2, and 46.8 % were acquired at 35 °C for methanol, ethanol, and acetone respectively. Therefore, acetone was selected as regenerative solvent for the sorbent.

3.7 Adsorption Isotherms

Adsorption isotherms investigation is one of most important factors for any heterogeneous sorbent in all chemical processes. The adsorption isotherms imply the partition of adsorbate molecules between the liquid sample solution and solid sorbent in the adsorption process. In fact, the adsorption isotherms refer to the chemistry of the adsorbent and adsorbate at a proper temperature. In order to study the adsorption isotherm of the process, the ubiquitous isotherms of Langmuir and Freundlich were considered at different

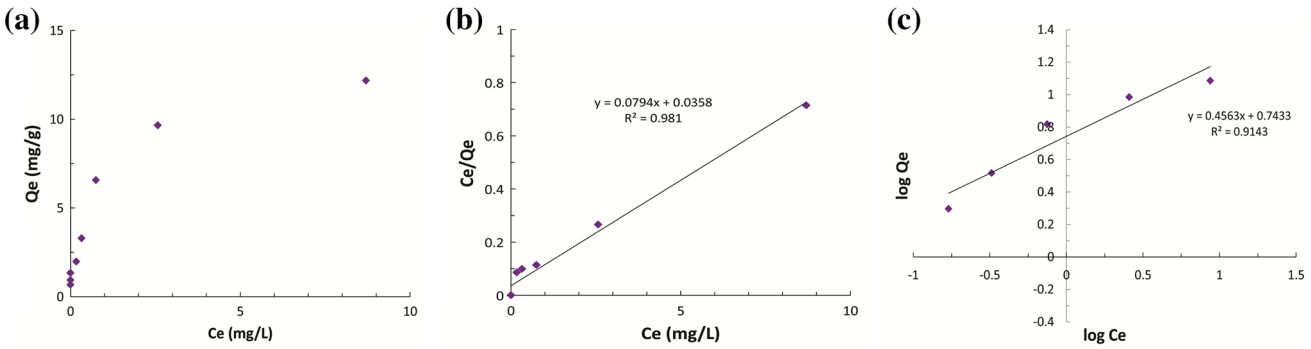

Fig. 7 The adsorption isotherms; Langmuir isotherm plots (**a**, **b**) and Freundlich isotherm plot (**c**) obtained at optimum conditions

Table 3 Isotherm parameters for adsorption of crystal violet (CV) onto the magnetic activated carbon at the optimum conditions

Dye	Langmuir isotherm					
	Q_{max} (mg g^{-1})	b (Lmg^{-1})	R^2	R_L	S_m^a	S_b^b
	12.59	2.218	0.981	0.004	0.005	0.020
CV	Freundlich isotherm					
	K_f	$1/n$	N	R^2	S_m	S_b
	5.537	0.456	2.192	0.9143	0.080	0.049

[a] Standard deviation of slope
[b] Standard deviation of intercept

concentrations in the range of 5–500 mg L^{-1} at optimum conditions. Langmuir isotherm consists of the monolayer adsorption on a homogenous adsorbent and has a rational basis. Each vacant site can only be occupied by one ion [27]. The Langmuir equation is as follows [28]:

$$C_e/Q_e = 1/(Q_m b) + C_e/Q_m \tag{10}$$

where Q_m is the saturation adsorption capacity (mg g^{-1}) and b is the constant related to the free energy of adsorption were obtained from the slope and the intercept of the equation. The plots of Q_i versus C_e, and C_e/Q_e versus C_e are shown in Fig. 7. The favorability of crystal violet adsorption onto the magnetic activated carbon can be calculated by dimensionless constant called separation factor, R_L (Eq. 9):

$$R_L = 1/(1 + bC_0) \tag{11}$$

In this equation C_0 (mg g^{-1}) is the highest initial ions concentration in adsorption isotherm studies. The value of R_L implies the unfavorable ($R_L > 1$), linear ($R_L = 1$), favorable ($0 < R_L < 1$), and irreversible ($R_L = 0$) types of the adsorption isotherm [2,9,29]. As the results indicate in Table 1, the values of R_L for two ions are $0 < R_L < 1$ which are favorable for adsorption isotherm.

The Freundlich isotherm is an empirical equation which is widely employed for numerous adsorption processes. The Freundlich isotherm was also applied for this study considering Eq. 10 as below:

$$Q_e = K_f C_e^{(1/n)} \tag{12}$$

This can be linearized as following:

$$\text{Log } Q_e = \log K_f + 1/\text{n} \log C_e \tag{13}$$

where the K_f is Freundlich constant related to the adsorbent capacity, and n is the constant indicative to the intensity of the adsorption process. The values of the constants, n and K_f, were calculated from the slope and the intercepts of the equation and shown in Table 3. The Langmuir and Freundlich isotherm plots are shown in Fig. 7. The Freundlich intensity constant of crystal violet was as $n > 1$ which show the significant adsorption of crystal violet in the proposed procedure even at high ion concentrations. The diagrams showed models were ideally fitted to the data of adsorption of crystal violet. Mean correlation coefficient of 0.981 was achieved for Langmuir isotherm plots. Moreover, Freundlich isotherm could satisfactorily depict crystal violet adsorption onto magnetic activated carbon.

4 Conclusions

The easily separable inexpensive magnetic activated carbon was synthesized and applied for removal of crystal violet, as a harmful compound for human health, from aqueous solution. The optimum conditions of 9.5, 25 °C, 36 min, 19.8 mg L^{-1}, and 52.8 mg, for pH, temperature, time, and initial dye concentration, and amount of sorbent were obtained respectively. Under optimum conditions, the maximum removal percent of 99.5 ± 0.2 was achieved experimentally which showed the high adsorption potential of the proposed sorbent. The adsorption isotherms studies showed favorable fitting of the process in Langmuir and Freundlich isotherms. Two statistical models of RSM and ANN were applied effectively to estimate the process with MAPE (%) of 0.59 and 0.38, and the determination coefficient of R^2 values of 0.9953 and 0.9980 respectively. The results confirmed that higher potential of ANN for prediction of the proposed method comparing to CCD. Furthermore, magnetic activated carbon, utilized in this study, can be properly used in industrial scale due to the advantages of easy separation, low-cost sorbent, and high percent of dye removal.

Acknowledgments The financial support of this project by Shahrekord University is appreciated. The authors were also partially supported by the Center of Excellence for Mathematics, Shahrekord University.

References

1. Puzyn, T.: Organic Pollutants Ten Years After the Stockholm Convention-Environmental and Analytical Update, vol. 472. InTech (2012)
2. Shirani, M.; Semnani, A.; Haddadi, H.; Habibollahi, S.: Optimization of simultaneous removal of methylene blue, crystal violet, and fuchsine from aqueous solutions by magnetic nay zeolite composite. Water Air Soil Pollut. **225**(8), 1–15 (2014). doi:10.1007/s11270-014-2054-2
3. Gözmen, B.; Kayan, B.; Gizir, A.M.; Hesenov, A.: Oxidative degradations of reactive blue 4 dye by different advanced oxidation methods. J. Hazard. Mater. **168**(1), 129–136 (2009)
4. Kalyani, K.; Balasubramanian, N.; Srinivasakannan, C.: Decolorization and COD reduction of paper industrial effluent using electro-coagulation. Chem. Eng. J. **151**(1), 97–104 (2009)
5. Morshedi, D.; Mohammadi, Z.; Akbar Boojar, M.M.; Aliakbari, F.: Using protein nanofibrils to remove azo dyes from aqueous solution by the coagulation process. Colloids Surf. B. Biointerfaces **112**, 245–254 (2013)
6. Alventosa-deLara, E.; Barredo-Damas, S.; Alcaina-Miranda, M.; Iborra-Clar, M.: Ultrafiltration technology with a ceramic membrane for reactive dye removal: optimization of membrane performance. J. Hazard. Mater. **209**, 492–500 (2012)
7. Wijannarong, S.; Aroonsrimorakot, S.; Thavipoke, P.; Sangjan, S.: Removal of reactive dyes from textile dyeing industrial effluent by ozonation process. APCBEE Procedia **5**, 279–282 (2013)
8. Dutta, S.; Parsons, S.A.; Bhattacharjee, C.; Bandhyopadhyay, S.; Datta, S.: Development of an artificial neural network model for adsorption and photocatalysis of reactive dye on TiO_2 surface. Expert Syst. Appl. **37**(12), 8634–8638 (2010). doi:10.1016/j.eswa.2010.06.090
9. Shirani, M.; Akbari, A.; Hassani, M.: Adsorption of cadmium(II) and copper(II) from soil and water samples onto a magnetic organozeolite modified with 2-(3,4-dihydroxyphenyl)-1,3-dithiane using an artificial neural network and analysed by flame atomic absorption spectrometry. Anal. Methods **7**(14), 6012–6020 (2015). doi:10.1039/C5AY01269D
10. Chakraborty, S.; Chowdhury, S.; Saha, P.: Artificial neural network (ANN) modeling of dynamic adsorption of crystal violet from aqueous solution using citric-acid-modified rice (*Oryza sativa*) straw as adsorbent. Clean Technol. Environ. Policy **15**(2), 255–264 (2013). doi:10.1007/s10098-012-0503-4
11. Bezerra, M.A.; Santelli, R.E.; Oliveira, E.P.; Villar, L.S.; Escaleira, L.A.: Response surface methodology (RSM) as a tool for optimization in analytical chemistry. Talanta **76**(5), 965–977 (2008). doi:10.1016/j.talanta.2008.05.019
12. Simić, V.M.; Rajković, K.M.; Stojičević, S.S.; Veličković, D.T.; Nikolić, N.Č.; Lazić, M.L.; Karabegović, I.T.: Optimization of microwave-assisted extraction of total polyphenolic compounds from chokeberries by response surface methodology and artificial neural network. Sep. Purif. Technol. (2016). doi:10.1016/j.seppur.2016.01.019
13. Podstawczyk, D.; Witek-Krowiak, A.; Dawiec, A.; Bhatnagar, A.: Biosorption of copper(II) ions by flax meal: empirical modeling and process optimization by response surface methodology (RSM) and artificial neural network (ANN) simulation. Ecol. Eng. **83**, 364–379 (2015). doi:10.1016/j.ecoleng.2015.07.004
14. Rahimpour, F.; Hatti-Kaul, R.; Mamo, G.: Response surface methodology and artificial neural network modelling of an aqueous two-phase system for purification of a recombinant alkaline active xylanase. Process Biochem. (2016). doi:10.1016/j.procbio.2015.12.018
15. Dil, E.A.; Ghaedi, M.; Ghaedi, A.; Asfaram, A.; Jamshidi, M.; Purkait, M.K.: Application of artificial neural network and response surface methodology for the removal of crystal violet by zinc oxide nanorods loaded on activate carbon: kinetics and equilibrium study. J. Taiwan Inst. Chem. Eng. (2015). doi:10.1016/j.jtice.2015.07.023
16. Sarve, A.; Sonawane, S.S.; Varma, M.N.: Ultrasound assisted biodiesel production from sesame (*Sesamum indicum* L.) oil using barium hydroxide as a heterogeneous catalyst: comparative assessment of prediction abilities between response surface methodology (RSM) and artificial neural network (ANN). Ultrason. Sonochem. **26**, 218–228 (2015). doi:10.1016/j.ultsonch.2015.01.013
17. Khayet, M.; Cojocaru, C.; Essalhi, M.: Artificial neural network modeling and response surface methodology of desalination by reverse osmosis. J. Membr. Sci. **368**(1–2), 202–214 (2011). doi:10.1016/j.memsci.2010.11.030
18. Sudamalla, P.; Saravanan, P.; Matheswaran, M.: Optimization of operating parameters using response surface methodology for adsorption of crystal violet by activated carbon prepared from mango kernel. Environ. Res. **22**(1), 1–7 (2012)
19. Singh, K.P.; Gupta, S.; Singh, A.K.; Sinha, S.: Optimizing adsorption of crystal violet dye from water by magnetic nanocomposite using response surface modeling approach. J. Hazard. Mater. **186**(2–3), 1462–1473 (2011). doi:10.1016/j.jhazmat.2010.12.032
20. Šafařík, I.; Nymburská, K.; Šafaříková, M.: Adsorption of water-soluble organic dyes on magnetic charcoal. J. Chem. Technol. Biotechnol. **69**(1), 1–4 (1997)
21. Kannan, N.; Veemaraj, T.: Removal of lead(II) ions by adsorption ontobamboo dust and commercial activated carbons—a comparative study. J. Chem. **6**(1), 247–256 (2009)
22. Shirani, M.; Ghaziaskar, H.S.; Xu, C.: Optimization of glycerol ketalization to produce solketal as biodiesel additive in a contin-

uous reactor with subcritical acetone using Purolite® PD206 as catalyst. Fuel Process. Technol. **124**(0), 206–211 (2014). doi:10.1016/j.fuproc.2014.03.007

23. Shakeri, S.; Ghassemi, A.; Hassani, M.; Hajian, A.: Investigation of material removal rate and surface roughness in wire electrical discharge machining process for cementation alloy steel using artificial neural network. Int. J. Adv. Manuf. Technol. (2015). doi:10.1007/s00170-015-7349-y
24. Salleh, M.A.M.; Mahmoud, D.K.; Karim, W.A.W.A.; Idris, A.: Cationic and anionic dye adsorption by agricultural solid wastes: a comprehensive review. Desalination **280**(1), 1–13 (2011)
25. Elemen, S.; Akçakoca Kumbasar, E.P.; Yapar, S.: Modeling the adsorption of textile dye on organoclay using an artificial neural network. Dyes Pigment. **95**(1), 102–111 (2012). doi:10.1016/j.dyepig.2012.03.001
26. Bingöl, D.; Hercan, M.; Elevli, S.; Kılıç, E.: Comparison of the results of response surface methodology and artificial neural network for the biosorption of lead using black cumin. Bioresour. Technol. **112**(0), 111–115 (2012). doi:10.1016/j.biortech.2012.02.084
27. Sohrabnezhad, S.; Pourahmad, A.: Comparison absorption of new methylene blue dye in zeolite and nanocrystal zeolite. Desalination **256**(1), 84–89 (2010)
28. Faghihian, H.; Moayed, M.; Firooz, A.; Iravani, M.: Synthesis of a novel magnetic zeolite nanocomposite for removal of Cs^{+} and Sr^{2+} from aqueous solution: kinetic, equilibrium, and thermodynamic studies. J. Colloid Interface Sci. **393**(0), 445–451 (2013). doi:10.1016/j.jcis.2012.11.010
29. Mohan, D.; Chander, S.: Single, binary, and multicomponent sorption of iron and manganese on lignite. J. Colloid Interface Sci. **299**(1), 76–87 (2006). doi:10.1016/j.jcis.2006.02.010